Retention of Adenovirus E19 Glycoprotein in the Endoplasmic Reticulum Is Essential to Its Ability to Block Antigen Presentation

By Josephine H. Cox, Jack R. Bennink, and Jonathan W. Yewdell

From the Laboratory of Viral Diseases, National Institute of Allergy and Infectious Diseases, National Institutes of Health, Bethesda, Maryland, 20892

Summary

The E3/19K glycoprotein of adenovirus functions to diminish recognition of adenovirus-infected cells by major histocompatibility complex class I-restricted cytotoxic T lymphocytes (CTLs) by binding intracellular class I molecules and preventing them from reaching the plasma membrane. In the present study we have characterized the nature of the interaction between E3/19K and the H-2K^d (K^d) molecule. An E3/19K molecule genetically engineered to terminate six residues from its normal COOH terminus (ΔE19), was found to associate with K^d in a manner indistinguishable from wild-type E3/19K. Unlike E3/19K, however, ΔE19 was transported through the Golgi complex to the plasma membrane, where it could be detected biochemically and immunocytochemically using a monoclonal antibody specific for the lumenal domain of E3/19K. Importantly, ΔE19 also differed from E3/19K in being unable to prevent the presentation of K^d-restricted viral proteins to CTLs. This is unlikely to be due to ΔE19 having a lower avidity for K^d than E3/19K, since ΔE19 was able to compete with E3/19K for K^d binding, both physically, and functionally in nullifying the E3/19K blockade of antigen presentation. These findings indicate that the ability of E3/19K to block antigen presentation is due solely to its ability to retain newly synthesized class I molecules in the endoplasmic reticulum.

M HC class I-restricted CTLs recognize virus-infected cells and release soluble factors that either lyse the cell or have direct or indirect antiviral activities. The specificity of triggering this response is conferred by the TCR, which binds class I molecules on the virus-infected cell complexed to linear determinants from viral proteins. Under normal conditions, these determinants are derived from newly synthesized viral proteins present in the cytosol of virus-infected cells (1–3).

Perhaps the most compelling evidence that CTLs are able to reduce the reproductive capacity of viruses is the existence of viral proteins, nonessential to viral replication, that diminish the presentation of viral antigens to CTLs. The best characterized of these proteins is the E3/19K glycoprotein (E19) encoded by some adenovirus serotypes. E19 is a resident endoplasmic reticulum (ER)[1] glycoprotein expressed early in adenovirus infection that forms a tight complex with most human MHC class I allomorphs, preventing them from reaching the cell surface. This prevents CTLs from recognizing viral proteins synthesized after synthesis of E19 has commenced (4–6), presumably because antigens processed from the cytosol must associate with newly synthesized class

I molecules in an intracellular location (7–9). The retention of E19 in the ER requires the presence of the six amino residues that constitute its cytosolic COOH terminus. These residues (DEKKMP) act as a positive signal for ER retention, since their transfer to the COOH terminus of other type I-anchored membrane glycoproteins confers ER retention (10).

Although adenovirus is a human pathogen, E19 can also bind some mouse class I MHC allomorphs (11). This is not totally unexpected given the close sequence homology between human and mouse class I molecules. The differential binding of E19 to mouse class I allomorphs has been exploited to determine that residues in or near the antigen binding groove of class I molecules can influence the ability of E19 to bind class I molecules in the ER (12, 13). This finding raises the possibility that E19 binds to this region of class I molecules, and perhaps prevents antigen association with class I molecules.

Previously, we showed that mouse cells infected with a vaccinia virus (Vac) recombinant expressing the E19 glycoprotein exhibit a deficit in presentation of newly synthesized proteins in association with some mouse class I allomorphs. The extent of the deficit correlated with the degree to which the allomorphs co-precipitated E19 from detergent extracts of ^{35}S-methionine-labeled cells, and was most pronounced with K^d, which bound E19 in an equimolar complex (6), and failed to reach the cell surface. These findings indicated

that proteins processed by the cytosolic processing pathway associate with newly synthesized class I molecules during their transport to the cell surface.

In the present study we further characterize the interaction of E19 with class I molecules. We have produced a vaccinia virus (Vac) recombinant expressing a truncated E19 molecule that is not retained in the ER but maintains a high affinity for K^d. Using this recombinant we show that the truncated E19 does not block the exocytosis of class I molecules, and does not affect the presentation of viral antigens processed by the cytosolic route.

Materials and Methods

Cells and Antibodies. Murine mastocytoma P815 (H-2^d) cells were maintained in RPMI supplemented with 7% (vol/vol) FCS, murine fibroblastoid L929 cells (H-2^k) in DMEM with 7% FCS, and hybridoma cells in IMDM with 7% FCS. The antibody-producing hybridomas, SF1-1.1.1 (HB159) (anti-K^d) and 16-1-11N (HB 16) (anti-K^k), were obtained from the American Type Culture Collection (Rockville, MD) and maintained in IMDM with 7% FCS.

Monoclonal Anti-E19 Antibody. Splenocytes derived from BALB/cByJ mice (The Jackson Laboratory, Bar Harbor, ME), immunized first with sonicated E19-Vac (6) -infected mouse spleen cells and 3 wk later with sonicated adenovirus 5–infected human KB cells, were fused with SP2 myeloma cells. An E19-specific antibody-producing hybridoma was identified by immunoperoxidase screening of E19-Vac-infected cells. After cloning, this hybridoma (Tw1.3) continued to produce an antibody of the γ3 subtype that specifically precipitated both E19 and ΔE19 (Fig. 1 *b*).

Immunofluorescence and Cytofluorography. For cytofluorography, cells were infected with Vac recombinants for 4 h at 37°C. Viable cells or cells fixed and permeabilized by brief incubation with 70% ethanol were washed twice and incubated with mAb diluted in PBS, 1% BSA, 1% azide at 4°C for 40 min. Cells were then washed twice with PBS, incubated at 4°C for 40 min with fluorescein-conjugated rabbit anti–mouse Ig (Dako Corp., Carpinteria, CA), washed twice, and their fluorescence quantitated using an Epics cytofluorograph (Coulter Electronics, Hialeah, FL). For immunofluorescence microscopy, infected P815 cells were centrifuged onto acid-cleaned 13-mm glass coverslips in a 24-well plate. After air drying, cells were fixed for 20 min in 0.5% (wt/vol) paraformaldehyde and permeabilized by the addition of 0.1% (wt/vol) saponin during all subsequent incubations. For colocalization studies with Con A, cells were incubated for 90 min at 4°C with Tw1.3, washed twice, and incubated for 90 min at 4°C with fluorescein-conjugated rabbit anti–mouse Ig alone or with rhodamine-conjugated Con A. For double immunofluorescence studies, cells were incubated with a rabbit antisera raised to MG160, a resident protein of the medial Golgi complex (GC) (14, 15), followed by fluorescein-conjugated goat anti–rabbit IgG. To block free antibody binding sites on the goat antibody, rabbit serum was added for 10 min at room temperature, followed by Tw1.3 anti-E19 antibody culture supernatant diluted 1:3. Finally, rhodamine-conjugated anti–mouse IgG was added. Coverslips were mounted in Mowiol-PBS containing 5% (wt/vol) 1,4 diazabicyclo[2.2.2]octane to retard fading. Cells were examined using an Axiophot photomicroscope (Carl Zeiss, Inc., Thornwood, NY) equipped with appropriate filters to gate red and green fluorescence. Images obtained with a 100× plan-neofluor objective were captured with a video camera (C2400-08 SIT; Hamamatsu, Hamamatsu City, Japan). After digital processing

with an image processor (DVS-3000; Hamamatsu), the images were transferred to a Macintosh II computer and further enhanced in the Macintosh II using the Adobe Photoshop program to change eight-bit grey scale images into eight-bit red or green images. The images were then printed separately or superimposed using a Sony Mavigraph color video printer.

Construction of Vaccinia Recombinants. To produce ΔE19-Vac, two synthetic oligonucleotides were used, a 30-base 5' primer corresponding to nucleotide 1394–1414 of the published E19 sequence (16) and encoding a SalI digestion site and Kozac sequence (17), and a 34-base 3' primer corresponding to E19 nucleotide 1856–1875 followed by nucleotides encoding two stop codons, NotI restriction site, and then 10 nucleotides corresponding to E19 nucleotide 1876–1885. Primers were used in the PCR using the pJC1 plasmid (6) containing the E19 gene. The PCR product was gel purified and digested with SalI and NotI restriction enzymes, and ligated into the SalI-NotI site of a derivative of pSC.11 modified to contain these sites to allow directional ligations (L. E. Eisenlohr, manuscript submitted for publication). Vaccinia recombinants were produced using this plasmid as described (6). The sequence of the ΔE19-Vac was confirmed by DNA sequence analysis of the plasmid DNA corresponding to the entire ΔE19 gene (data not shown).

Cell Labeling and Immunoprecipitation. Cells infected with vaccinia recombinants were incubated in methionine-free medium for 30 min at 37°C and radiolabeled for 10 min at 37°C by incubating cells at a concentration of 10^7 cells/ml with 100–200 μCi ^{35}S-methionine (Amersham Corp., Arlington Heights, IL). In pulse-chase experiments, cells were incubated after radiolabeling with medium supplemented with 5 mg/ml methionine for the indicated times at 37°C. For each sample, at least 2 × 10^6 labeled cells were lysed in PBS (pH 8.0), containing 0.5% NP-40, 1 mM PMSF at 4°C for 20 min. Extracts were centrifuged at 15,000 *g* and the supernatants incubated with protein A–Sepharose beads (Pierce Chemical Co., Rockford, IL) loaded with mAbs. Half of the immunoprecipitates were digested overnight at 32°C with endo H (Boehringer Mannheim Biochemicals, Indianapolis, IN). Immunoprecipitates were analyzed on 12% polyacrylamide gels using the buffer system of Laemmli (18). Gels were fixed and incubated with Amplify (Amersham Corp.) before drying under vacuum. Dried gels were exposed to preflashed Kodak XAR-5 film at −70°C.

Cytotoxicity Assay. P815 (2 × 10^6) cells were infected with vaccinia recombinants for 3 h and labeled for 1 h with Na^{51}CrO$_4$ (Amersham Corp.). Radiolabeled cells were incubated for 4 h at 37°C with antiinfluenza effector cells. Effector cells were obtained from cultures of splenocytes from influenza A/Puerto Rico/8/34 (H1N1) (PR8) hemagglutinin (H1-vac), nucleoprotein (NP-vac), nonstructural 1 (NS1-vac), or basic polymerase 2 (PB2-vac) recombinant vac-immunized BALB/cByJ mice restimulated in vitro with PR8 (19). The amount of ^{51}Cr released into the medium was determined by gamma radiation counting. Lysis of uninfected target cells ranged from 2 to 18% and was subtracted from all values. Experimental values represent the average of the triplicates; all values had a SEM of <4% of the specific release. The percent ^{51}Cr release was calculated as follows: 100× [(experimental cpm − spontaneous [no splenocytes] cpm)/(total [detergent] cpm − spontaneous cpm)]. Spontaneous release values were always <25% of total release.

Lactoperoxidase Iodination. Cells (10^7) infected with vac recombinants for 6–7 h were washed three times in PBS and resuspended in 0.8 ml PBS supplemented with 5 mM glucose, 1 mCi Na^{125}I (New England Nuclear, Boston, MA), 1 U/ml lactoperoxidase, and 5 U/ml glucoseoxidase. After a 5–15-min incubation at room temperature, an additional 1 U/ml lactoperoxidase and 5 U/ml

glucoseoxidase was added. Cells were then incubated for a further 15 min at room temperature, washed twice in PBS, 10 mM NaI, lysed in extraction buffer, and the extracts immunoprecipitated as described above.

Results

Production and Characterization of ΔE19-Vac and an E19-specific mAb. To examine whether E19 blocks antigen association with K^d requires the uniform expression of high levels of E19 nonconstitutively in target cell populations. The expression vector most suited for this purpose is Vac, which also provides the advantage of allowing coexpression of additional foreign proteins by simply co-infecting cells with multiple Vac recombinants. We therefore constructed a Vac recombinant that expresses an E19 glycoprotein without the six COOH-terminal amino acids required for ER retention (ΔE19-Vac). A rabbit antiserum raised to a synthetic peptide corresponding to the 15 COOH-terminal amino acids of E19 that efficiently precipitates E19 failed to precipitate ΔE19 from ^{35}S-methionine-labeled ΔE19-Vac-infected P815 cells (Fig. 1 *a*). This confirmed that the COOH terminus was altered in ΔE19, and indicated that we could not use this antiserum to characterize ΔE19-Vac. To detect ΔE19 we produced a B cell hybridoma (Tw1.3) secreting a mouse mAb of the γ3 subtype that recognized both E19 and ΔE19 (see Materials and Methods). As seen in Fig. 1 *b*, the Tw1.3 mAb precipi-

tated both E19 and ΔE19 from detergent extracts of ^{35}S-methionine-labeled ΔE19-Vac and E19-Vac-infected cells, respectively, as determined by SDS-PAGE analysis of precipitates. This also revealed that ΔE19 migrated slightly faster than E19, which is consistent with its COOH-terminal deletion. The antibody is specific for the lumenal domain of E19, since, as described below, it binds to viable cells expressing ΔE19 on the plasma membrane.

The Tw1.3 mAb precipitated from E19-Vac-infected cell extracts an additional protein with an apparent molecular mass of 88 kD (Fig. 1 *c*, lane *3*). This is a cellular protein, since it was also specifically precipitated from uninfected cells (Fig. 1 *c*, lane *2*). It is potentially of great interest as it could represent a cellular homologue of E19. We have not been able, however, to demonstrate that this protein interacts with class I molecules, since class I molecules do not co-precipitate with the protein (the expected location of class I heavy chains can be determined from comparison with lane *1*, which represent immunoprecipitation with a K^d-specific mAb), even after chemical crosslinking of detergent extracts (not shown). It does not represent the 88-kD class I–associated protein identified by Degen and Williams (20) (Williams, D. B., personal communication). The protein might be expressed only at low steady-state levels in cells, since in indirect immunofluorescence, the Tw1.3 mAb does not stain uninfected cells above background levels obtained in the absence of a first antibody. It remains to be established whether the reactivity of 88-kD protein with Tw1.3 is fortuitous or indicates a true functional or evolutionary relationship with E19.

Immunolocalization of E19 and ΔE19. The cellular localization of ΔE19 and E19 in Vac recombinant–infected P815 cells was examined using the Tw1.3 mAb in indirect double immunofluorescence of fixed and permeabilized cells attached to coverslips. In E19-vac-infected cells, the Tw1.3 mAb stained the nuclear membrane and cytoplasmic structures (Fig. 2 *a*, *left*, red staining). A similar pattern was observed using rhodamine-Con A, which predominantly stains the ER by virtue of it specificity for terminal mannose residues (Fig. 2 *a*, *right*, green staining). The staining of Tw1.3 and Con A was largely co-incident as indicated by the yellow color obtained when superimposing the two images (Fig. 2 *a*, *middle*). To determine if E19 was also present in the GC, cells were double stained with Tw1.3 and a rabbit antiserum specific for a resident protein of the medial GC (14, 15). The GC in P815 cells centrifuged onto coverslips appears as small green punctate structures (Fig. 2, *b* and *c*, *right*). Little of this stain colocalized with TW1.3 in E19-Vac-infected cells (Fig. 2 *b*, *middle*). By contrast, TW1.3 clearly colocalized with the anti-GC antiserum (Fig. 2 *c*, *middle*) in ΔE19-Vac-infected cells, in addition to staining the ER (Fig. 2 *c*, *left*). This analysis suggested that while E19 was restricted to pre-GC compartments, ΔE19 was transported to the GC.

To quantitatively determine whether ΔE19 was transported to the cell surface, L929 cells were infected with E19-Vac or ΔE19-Vac for 5 h, stained with Tw1.3, and analyzed using a cytofluorograph (Table 1). Using viable cells, Tw1.3 bound above background levels to ΔE19-Vac-, but not E19-Vac-infected cells. The failure to detect E19 on E19-Vac-infected cells is
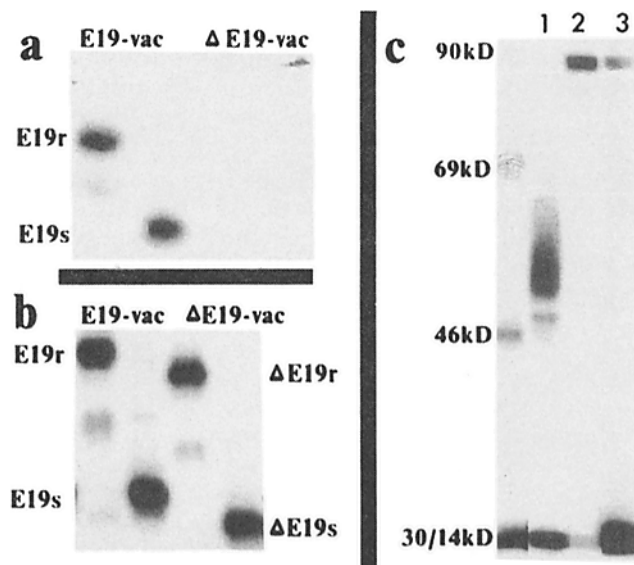

Figure 1. Characterization of anti E19 mAb. (*a* and *b*) P815 cells were infected with E19-Vac or ΔE19-Vac for 2 h and labeled for 10 min in ^{35}S-methionine. Detergent extracts were immunoprecipitated with protein A–Sepharose beads that had been loaded with (*a*) a rabbit antiserum specific for the COOH terminus of E19 or (*b*) Tw1.3 anti-E19 mAb. Immunoprecipitates were digested with endo H as indicated and analyzed by SDS-PAGE. Endo H–resistant (E19r, ΔE19r) and Endo H–sensitive (E19s, ΔE19s) forms of the E19 protein are indicated. (*c*) Similarly, uninfected cells (lanes *1* and *2*) or E19-vac infected cells (lane *3*) were labeled for 3 h with ^{35}S-methionine and detergent extracts were immunoprecipitated with anti-K^d class I mAb (lane *1*) or Tw1.3 anti-E19 mAb (lanes *2* and *3*).
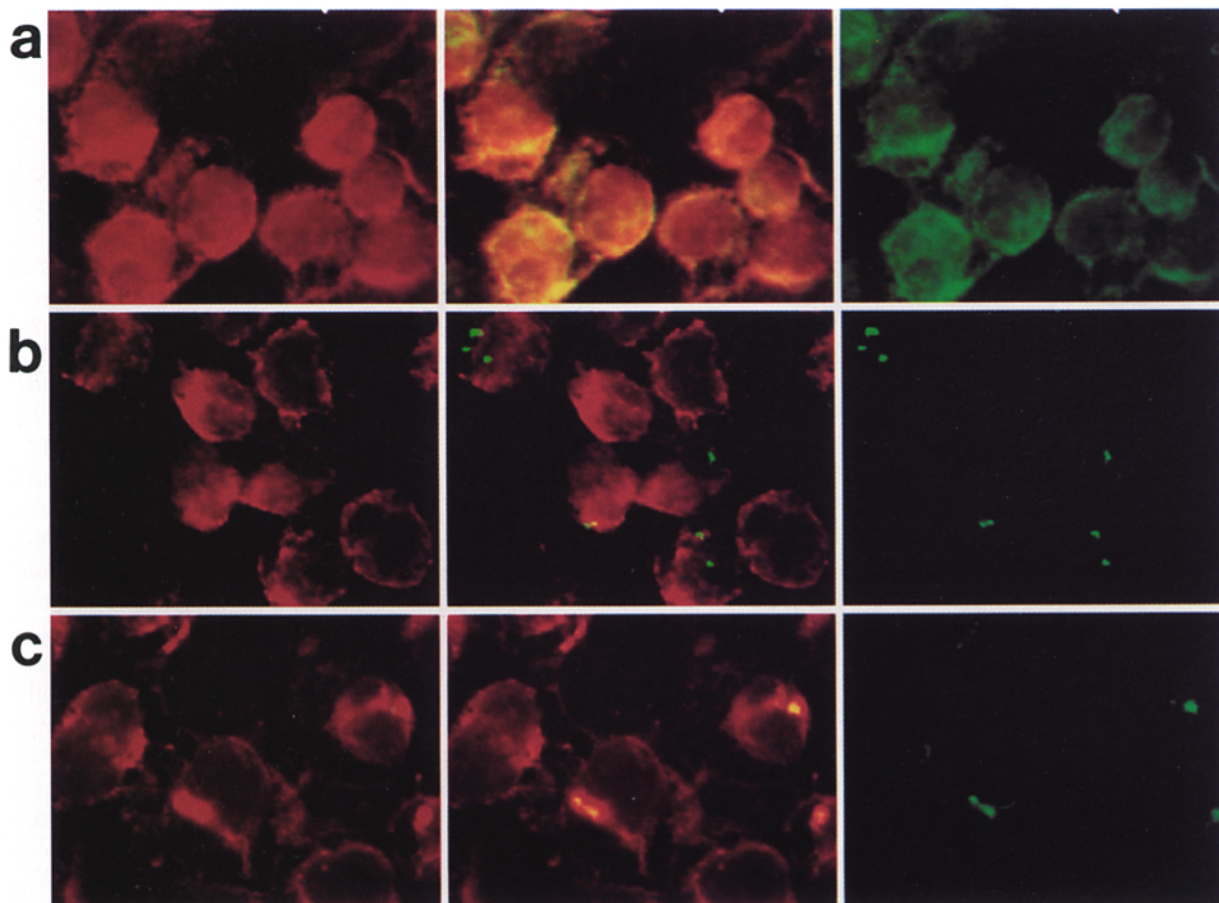
Figure 2. Immunofluorescence localization of E19 and ΔE19. P815 cells infected with E19-Vac (*a* and *b*) or ΔE19-Vac (*c*) for 5 h were fixed and permeabilized before double staining with Tw1.3 anti-E19 mAb and Con A (*a*) or with Tw1.3 and a rabbit antiserum specific for a resident protein of the medial GC (*b* and *c*). The green color (*right*) represents staining with the Mg160 anti-Golgi antibody (*b* and *c*) or Con A (*a*), the red color (*left*) represents staining with anti-E19. (*Middle*) The green and red images have been merged to yield yellow color where staining coincides.

not due to low levels of expression, since ethanol-permeabilized cells actually bound more Tw1.3- than ΔE19-Vac-infected cells. Thus, ΔE19 but not E19 is transported to the cell surface of Vac recombinant–expressing cells.

In the same experiment, we examined the ability of E19 and ΔE19 to block the surface expression of newly synthesized K^d molecules. Infection of L929 cells (H-2^k) with a Vac recombinant–expressing K^d (K^d-Vac) (21) resulted in the ex-

Table 1. *Transport of Newly Synthesized K^d Is Not Inhibited by the ΔE19 Protein*

	Immunofluorescence percent positive (mean intensity)			
	Live cells		Permeabilized	
Coinfection of L929 cells	K^d	E19	K^d	E19
Kd-Vac	96.1 (15.5)	2.7 (7.8)	88.2 (8)	4.3 (6.4)
Kd-Vac + E19-Vac	3.0 (6.6)	11.6 (15.4)	81.2 (9.8)	89.4 (13)
Kd-Vac + ΔE19-Vac	86.2 (9.4)	49.5 (6)	86.1 (10)	80.4 (9.6)
E19-Vac	1 (6.7)	2.7 (9)	4.2 (9.2)	93.7 (12.5)
ΔE19-Vac	1.2 (9)	54 (7)	3.7 (8.4)	83 (8.3)

L cells were infected with Vac recombinants for 4 h, and live cells and cells fixed and permeabilized in 70% ethanol were stained with anti-K^d SF1-1.1.1 or the Tw1.3 and analyzed via cytofluorography.

pression of K^d on 96% of the cells (Table 1). K^d was not detected on the surface of cells co-infected with K^d-Vac and E19-Vac, while it was detected in cells co-infected with K^d-Vac and ΔE19-Vac, albeit at reduced levels. The lack of K^d surface expression in cells co-infected with E19-Vac and K^d-Vac is not due to low expression of the K^d gene, since permeabilized cells expressed similar amounts of K^d as cells infected only with K^d-Vac, or with K^d-Vac and ΔE19-Vac. The finding that the surface expression of newly synthesized K^d was not significantly inhibited by ΔE19-vac was further confirmed by the immunoprecipitation of K^d from L929 cells co-infected with K^d-Vac and ΔE19-Vac, whose cell surface proteins were labeled by lactoperoxidase catalyzed iodination (data not shown).

Biochemical Analysis of ΔE19 Intracellular Transport and Binding to K^d. To biochemically characterize the intracellular trafficking of E19 and ΔE19, ^{35}S-methionine pulse-labeled P815 cells were chased for various times at 37°C, detergent extracted, and immunoprecipitated with Tw1.3 anti-E19 mAb or with an anti-H-2K^d mAb. Before analysis by SDS-PAGE, half the samples were treated with endo H to remove the simple oligosaccharides characteristic of glycoproteins before they are modified by enzymes that reside in the medial GC. Deglycosylation by endo H results in an easily detectable increase in the mobility of K^d and E19 in SDS-PAGE, and indicates proteins in a post-ER compartment. The resistance of proteins to this mobility shift suggests that they have been transported to or through the medial GC.

Immediately after pulse-labeling, ΔE19 was completely sensitive to endo H digestion (Fig. 3). With increasing times after the pulse, a subpopulation of ΔE19 became less sensitive to digestion with endo H, indicating that at least a portion the ΔE19 can transit through the Golgi. As is typical of proteins with mature oligosaccharides, endo H–resistant ΔE19 migrated with slightly lower mobility than ΔE19 with less mature oligosaccharides. In contrast, all the newly synthesized E19 remained sensitive to endo H digestion over the entire 8-h chase period (Fig. 3).
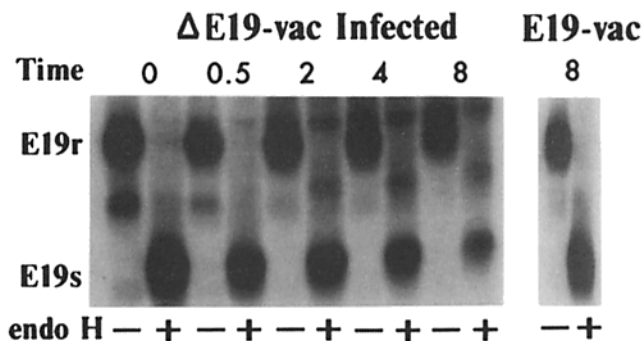

Figure 3. Transport of ΔE19 protein. P815 cells were infected with E19-Vac or ΔE19-Vac for 2 h and labeled for 10 min in ^{35}S-methionine, and chased at 37°C for the times indicated. Detergent extracts were immunoprecipitated with protein A–Sepharose beads that had been loaded with Tw1.3 anti-E19 mAb. Immunoprecipitates were digested with endo H as indicated and analyzed by SDS-PAGE. E19r; endo H–resistant E19, E19s; endo H–sensitive E19.
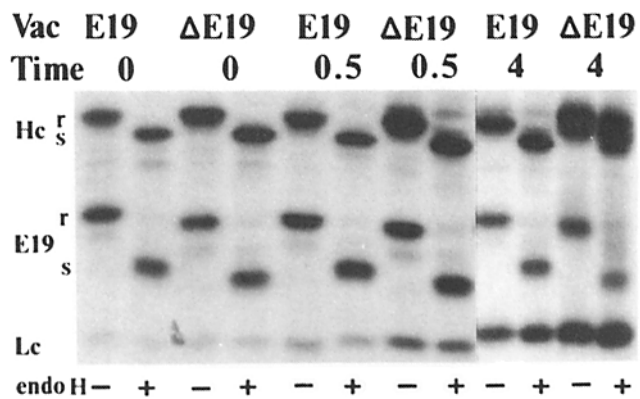

Figure 4. Transport of class I K^d protein. P815 cells were infected with E19-Vac or ΔE19-Vac for 2 h and labeled for 10 min in ^{35}S-methionine, and chased at 37°C for the times indicated. Detergent extracts were immunoprecipitated with protein A–Sepharose beads that had been loaded with anti-K^d class I mAb. Immunoprecipitates were digested with endo H as indicated and analyzed by SDS-PAGE. Hc, Heavy chain class I; Lc, β_2-microglobulin; s, endo H sensitive; r, endo H resistant.

Immunoprecipitation of detergent lysates with anti-K^d revealed that newly synthesized ΔE19, like E19, complexed within the 10-min pulse to newly synthesized K^d, and remained bound in an $\sim$1:1 ratio over the 4-h pulse period (Fig. 4). β_2-microglobulin was co-precipitated from both E19-Vac- and ΔE19-Vac-infected cells in increasingly greater quantities after labeling. Most importantly, K^d synthesized in E19-Vac-infected cells remained sensitive to endo H digestion over the 4-h chase, while K^d precipitated from ΔE19-Vac became endo H resistant beginning within 30 min after labeling, and increasingly over the next 3.5 h. K^d in cells infected with a control Vac recombinant became almost completely resistant to endo H digestion within 1 h of synthesis (not shown). Since similar amounts of K^d and E19 were precipitated from E19-Vac- and ΔE19-Vac-infected cells, these findings strongly suggest that K^d associated with ΔE19 is transported through the GC.

To further examine the surface expression of E19 and ΔE19, cells were surface iodinated 7 h after infection with ΔE19-Vac and detergent extracts immunoprecipitated with the Tw1.3 mAb. Immunoprecipitates were then treated with endo H or left untreated, and analyzed by SDS-PAGE. As seen in Fig. 5, iodinated ΔE19 was easily detected by this method. To determine whether this labeled pool of ΔE19 was truly present on the cell surface and not in an intracellular location, ΔE19-Vac-infected cells were incubated with brefeldin A (BFA) to prevent the surface expression of ΔE19 (8). In this case far less ΔE19 was iodinated. This was due to the intracellular location of ΔE19 in these cells, not low levels of ΔE19 expression, since labeling of ΔE19 was completely restored by removing the BFA and incubating cells for 60 min at 37°C in the presence of protein synthesis inhibitors to prevent synthesis of additional ΔE19. It can also be seen in Fig. 5 that only low levels of E19 were radioiodinated on E19-Vac-infected cells. This almost certainly represents intra-

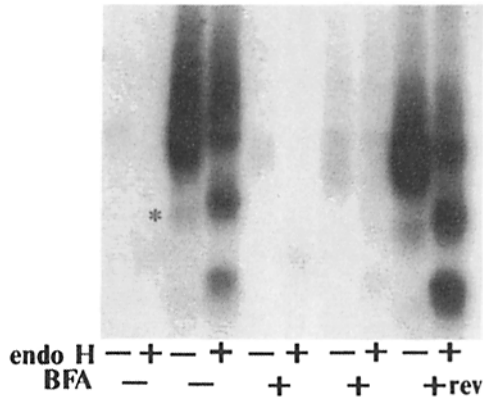endo H — + — + — + — + — +
BFA — — + + +rev

Figure 5. Surface iodination of ΔE19. P815 cells infected with Vac recombinants for 6–7 h were surface radioiodinated using lactoperoxidase. Cells were incubated where indicated with BFA from the time of infection. In the last two lanes, BFA was removed from cells that were incubated for another 1 h at 37°C in the presence of anisomycin at 25 µg/ml to block additional protein synthesis. Detergent lysates were immunoprecipitated using protein A–Sepharose beads that had been preloaded with Tw1.3 anti-E19 mAb. Immunoprecipitates were digested with endo H as indicated, and analyzed by SDS-PAGE.

Table 2. *ΔE19 Does Not Inhibit the Presentation of Influenza Virus Antigens*

Coinfection of P815 cells	Restriction	Percent specific ^{51}Cr release	
H1-Vac + E19-Vac	K^d	9	10
H1-Vac + ΔE19-Vac		64	49
H1-Vac + RSV-Vac		66	45
NP-Vac + E19-Vac	K^d	9	3
NP-Vac + ΔE19-Vac		75	56
NP-Vac + RSV-Vac		64	55
PB2-Vac + E19-Vac	D^d	35	17
PB2-Vac + ΔE19-Vac		36	9
PB2-Vac + RSV-Vac		29	13
NS1-Vac + E19-Vac	L^d	22	10
NS1-Vac + ΔE19-Vac		49	29
NS1-Vac + RSV-Vac		51	27

P815 cells were co-infected for 4 h at 37°C with 20 PFU per cell of E19-Vac, ΔE19-Vac, or respiratory synctial virus-Vac (RSV-Vac), and Vac recombinants expressing the influenza virus genes encoding either nucleoprotein (NP-Vac) or hemagglutinin (H1-Vac). Na^{51}CrO$_4$-labeled cells were incubated for 4 h at 37°C with antiinfluenza effector cells; experimental values represent the average of triplicates. E/T ratios were 58:1 and 7:1, respectively.

cellular E19, since similar amounts of E19 were radioiodinated in E19-Vac cells treated with BFA. Thus, these findings confirm that E19 is confined to intracellular compartments, while ΔE19 is able to reach the cell surface.

In addition to a major band migrating with the mobility expected for ΔE19, a minor radioiodinated species migrating with a mobility intermediate between glycosylated and deglycosylated E19 was precipitated by Tw1.3 (marked in Fig. 5 by an asterisk). A band of a similar mobility was apparent at early chase times in ^{35}S-methionine-labeling experiments (Fig. 3). The disappearance of this band upon endo H treatment of ^{35}S-methionine-labeled lysates (Fig. 3) suggests that this species represents ΔE19 containing only one of the two oligosaccharides normally added to E19.

Treatment of radioiodinated ΔE19 immunoprecipitates resulted in three bands, corresponding to ΔE19 with two, one, or zero oligosaccharides. Note that endo H–treated ΔE19 with a single oligosaccharide migrated with a lower mobility than the adjacent band in the non–endo H–treated lane, which is consistent with expected mobility difference between ΔE19 with a mature vs. immature oligosaccharide. This mobility difference indicates that this species is derived from ΔE19 containing two oligosaccharides. At least a portion of ΔE19 completely deglycosylated by endo H must also be derived from ΔE19 containing two oligosaccharides since there is more of this material than of the singly glycosylated, non–endo H–treated ΔE19. Thus, ΔE19 is able to reach the cell surface with one or both of its oligosaccharides in immature form.

Expression of ΔE19 Protein Does Not Affect Antigen Presentation. Four influenza virus proteins are recognized by CTL from H-2^d mice: hemagglutinin (HA) and nucleoprotein (NP) are recognized in association with K^d, nonstructural 1 (NS1) with L^d, and basic polymerase 2 (PB2) with D^d

(19). We previously found that co-infection of cells with E19-Vac and Vac recombinants expressing the individual viral proteins results in complete inhibition of presentation of HA and NP, partial inhibition of NS1, and very slight inhibition of PB2. To establish whether the ΔE19 protein behaved in a similar fashion, we repeated this experiment using ΔE19-Vac and CTL specific for the individual influenza virus antigens. ΔE19 did not inhibit the presentation of any of the influenza virus antigens, since cells co-infected with ΔE19-Vac were lysed at similar levels as cells co-infected with a control Vac recombinant expressing a protein from respiratory syncytial virus (Table 2). In the same experiment, E19 behaved as previously observed, efficiently blocking presentation of K^d-restricted HA and NP, partially blocking L^d-restricted NS-1, and not affecting D^d-restricted PB2.

A trivial explanation for the failure of ΔE19 to block antigen presentation of HA and NP is that it forms a more tenuous complex with K^d than does E19. Although this did not seem likely based on the equal co-precipitation of E19 and ΔE19 with K^d, it was important to demonstrate that ΔE19 could compete with E19 for binding of K^d, nullifying the E19 blockade of antigen presentation. This was accomplished by co-infecting cells with E19-Vac, ΔE19-Vac, and Vac recombinants expressing HA or NP. As seen in Table 3, co-infection with ΔE19-Vac completely restored the presentation of HA or NP. The recovery of antigen presentation is specifically mediated by ΔE19, and is not simply attributable

Table 3. *ΔE19 Protein Competes with E19 Protein for the Binding Site on Mouse K^d*

Co-infection of P815 cells	Percent specific ^{51}Cr release	
NP-Vac	69	52
NP-Vac + E19-Vac	22	10
NP-Vac + E19-Vac + ΔE19-Vac	58	42
NP-Vac + E19-Vac + RSV-Vac	10	5
H1-Vac	57	25
H1-Vac + E19-Vac	8	10
H1-Vac + E19-Vac + ΔE19-Vac	59	34
H1-Vac + E19-Vac + RSV-Vac	15	2

P815 cells were co-infected for 4 h at 37°C with 5 PFU per cell of E19-Vac, 20 PFU/cell of Vac recombinants expressing the influenza virus genes encoding either nucleoprotein (NP-Vac) or hemagglutinin (H1-Vac), and 100 PFU per cell of either ΔE19-Vac or RSV-Vac. Na^{51}CrO$_4$-labeled cells were incubated for 4 h at 37° with antiinfluenza effector cells; experimental values represent the average of triplicates. E/T ratios were 80:1 and 9:1, respectively.

to the effects of Vac superinfection, since co-infection with a similar dose of a control Vac recombinant had no effect on antigen presentation. Thus, these finding suggest that E19 does not block antigen association with class I molecules.

Intracellular Dimerization of E19 and ΔE19. It is likely that E19 exists in cells as multimers, since a subpopulation mi-

Figure 6. ΔE19 and E19 proteins can form heterodimers. P815 cells were infected for 3 h at 37°C with E19-Vac or Δ19-Vac alone, or co-infected at the indicated ratios. Cells were labeled for 10 min in ^{35}S-methionine, and extracted and immunoprecipitated with protein A–Sepharose beads loaded with Tw1.3 anti-E19 mAb (a) or anti-K^d class I mAb (b). Half of the immunoprecipitates were digested with endo H as indicated, and analyzed by SDS-PAGE under nonreducing conditions. *(Inset)* ww, wild-type E19 homodimer; wΔ, wild-type and ΔE19 heterodimer; ΔΔ, ΔE19 homodimer; *immunoprecipitated with anti-E19 mAb; **immunoprecipitated with anti-K^d mAb.

grates as dimers when analyzed in SDS-PAGE under non-reducing conditions. It was therefore possible that the effect of ΔE19 on E19-mediated blockade of antigen presentation was due to the formation of mixed dimers unable to bind to K^d. To examine this possibility, we characterized the ability of E19 and ΔE19 to form mixed dimers. In P815 cells infected with E19-Vac or ΔE19-Vac alone, the monomeric and dimeric forms of the respective proteins precipitated by Tw1.3 from pulse-labeled extracts could be completely distinguished from each other based on the higher mobility of ΔE19 (Fig. 6 a). In cells co-infected with equal doses of E19-Vac and ΔE19-Vac, a third band, presumably a heterodimer, was present halfway between the observed bands of the E19 and ΔE19 dimers. The heterodimer was more clearly visible after deglycosylation by endo H digestion, which is expected since oligosaccharides generally decrease the sharpness of protein migration in SDS-PAGE. The proportion of each of the species in cells infected under these conditions, or with 10-fold excess of one of the recombinants, approximates a binomial distribution of the three species, which suggests that E19 and ΔE19-Vac randomly associate with each other.

In parallel, extracts prepared from co-infected cells were immunoprecipitated with a K^d-specific mAb (Fig. 6 b). Both monomeric and dimeric forms of the E19 and ΔE19 were co-precipitated with K^d. Most importantly, heterodimers formed between the E19 and ΔE19 protein were also present, and therefore are fully capable of binding to class I molecules. Therefore, the observed competition between ΔE19 and E19 in blocking antigen presentation cannot be ascribed to the formation of heterodimers incapable of binding to K^d.

Discussion

The goal of the present study was to determine whether E19 blocks the association of antigen with class I molecules. Our strategy was to engineer a modified E19 glycoprotein that maintains its binding to class I molecules but is no longer retained in the ER. It had been shown previously that retention of E19 in the ER could be abrogated by altering residues in the COOH terminus of E19, a portion of the molecule that is believed to reside in the cytosol (22, 23). As removal of the entire cytosolic domain of E19 was found to reduce its binding to class I molecules (24), it was important to make a less severe alteration. There is some controversy regarding the exact features of cytosolic domain that confer ER retention. A recent report, however, clearly demonstrated that transfer of the six terminal residues of E19 to other membrane glycoproteins greatly retarded their exit from the ER (10). We therefore decided to delete only the six terminal residues from E19 in creating the ΔE19 protein.

By immunochemical and biochemical analysis, we demonstrated that ΔE19 is transported to the plasma membrane, confirming the importance of the cytosolic COOH-terminal residues in mediating ER retention. Some of the cell surface ΔE19 contained carbohydrates sensitive to digestion with endo H. This indicates either that the oligosaccharides are partially resistant to modification by enzymes in the GC, or that a subpopulation of ΔE19 does not traverse the entire GC. The
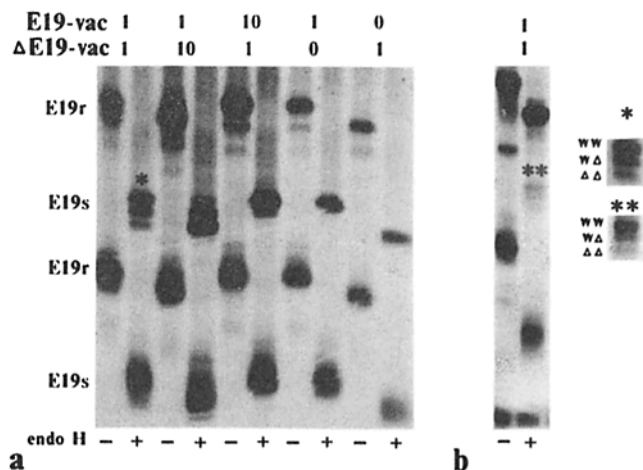
existence of surface ΔE19 with one endo H–sensitive and one endo H–resistant oligosaccharide indicates that the first mechanism accounts for some, if not all, of the oligosaccharide heterogeneity. The failure of GC enzymes to modify ΔE19 oligosaccharides is probably unrelated to its association with class I molecules, since we have observed a similar heterogeneity in L929 cells, which do not have class I molecules that tightly associate with ΔE19 or E19 (our unpublished results). Observations of similar heterogeneity in secreted forms of E19 expressed by insect cells, which do not possess MHC genes, support this conclusion (25). Instead, it is more likely that failure of GC enzymes to modify ΔE19-associated oligosaccharides is due to an intrinsic limit to their accessibility, perhaps because they are located in a more internal position after the assembly of ΔE19 into oligomers.

The maturation of E19-associated oligosaccharides, while incomplete, still serves as a measure of E19 export from the ER. By this criteria, ΔE19 is transported relatively slowly from the ER, with a half time of ~4 h. The half time of K^d acquisition of endo H resistance in ΔE19-Vac-infected cells demonstrated similar kinetics. This represents an ~10-fold increase over the half time of K^d export in Vac-infected cells, and indicates that ΔE19 remains complexed with K^d at least until K^d has passed through the medial GC.

This latter point bears on a question central to the interpretation of the inability of ΔE19 to block antigen presentation: how tight is the association of ΔE19 with K^d in the compartment where antigen association normally occurs? Two findings suggest that ΔE19 binds K^d with a similar avidity as E19 in early exocytic compartments. First, similar amounts of E19 and ΔE19 co-precipitate with K^d. Second, ΔE19 is able to compete with E19 both biochemically for K^d binding, and functionally, to reverse the effect of E19 on antigen presentation. Thus, it appears that ΔE19 binds to K^d with high affinity at least until the complex has passed through the medial GC. The stability of the complex during the latter stages of exocytosis remains to be established. As it is believed that antigens associate with class I molecules in an exocytic compartment proximal to the medial GC (6–9), it seems unlikely that the possible dissociation of ΔE19 from K^d in a late exocytic compartment would account for its failure to block antigen association. Ultimately, however, to definitively establish whether E19 blocks association of antigen with class I molecules will require direct examination of the peptide binding capacity of E19–class I complexes.

If ΔE19 remains in a tight complex with class I molecules at the cell surface, this would mean that E19 binding does not interfere with the interaction of class I molecules with the TCR. This would suggest that class I heavy chains are able to interact with at least four proteins simultaneously, the TCR, CD8, β_2-microglobulin, and E19. In this case, as the polymorphic residues in the $\alpha2$ domain that influence the affinity of E19 for mouse class I molecules are likely to be in close proximity to the TCR, it would further imply that these residues do not contact E19, but act by inducing conformational alterations in other regions of the heavy chain.

A recent study determined that E19 binding and rapid export from the ER of a series of K^d-K^k chimeric molecules coordinately mapped to five polymorphic residues in the first half of the $\alpha2$ domain (13). Based on this finding, it was proposed that E19 interferes with class I export by either affecting class I assembly, or by interfering with the interaction of class I molecules with accessory molecules that positively influence class I transport. Given the apparently normal binding of ΔE19 to K^d, the transport of ΔE19-K^d complexes to the cell surface and their recognition by CTL strongly argue that E19 blocks class I transport solely by virtue of its cytosolic ER retention sequence.

If E19 binds to class I molecules in a fundamentally different manner than CD8, β_2-microglobulin, antigenic peptides, or the TCR, from which cellular gene is E19 derived? E19 appears to have its origins among the Ig superfamily of genes, with whose members it shares a tenuous homology (26). Protein or DNA sequence analysis of the 88-kD protein that reacts with the Tw1.3 mAb could reveal that it is the cellular homologue of E19. Although this protein has no apparent role in class I assembly or transport, there is no guarantee that cellular descendents of the E19 ancestor will have any such function.

There are three general possibilities for the function of the modern cellular descendent(s) of the putative E19 ancestor. It might have nothing to do with class I assembly and transport, it might be one of the gene products known (20) or suspected (27) to interact with class I during exocytosis, or its interaction with class I genes could remain to be characterized. Regarding the latter possibility, it is clear that we are only beginning to understand the subtleties in the assembly and transport of class Ia molecules. Furthermore, the MHC encodes many class Ib molecules whose characteristics and functions are unknown, and that probably interact with a number of undiscovered MHC and non-MHC gene products, one of which could be descended from the progenitor of E19.

References

1. Townsend, A., and H. Bodmer. 1989. Antigen recognition by class I-restricted T lymphocytes. *Annu. Rev. Immunol.* 7:601.
2. Yewdell, J.W., and J.R. Bennink. 1990. The binary logic of antigen processing and presentation to T cells. *Cell.* 62:203.
3. Braciale, T.J., and V.L. Braciale. 1991. Antigen presentation: structural themes and functional variations. *Immunol. Today.* 12:124.
4. Tanaka, Y., and S.S. Tevethia. 1988. Differential effect of adenovirus 2 E3/19K glycoprotein on the expression of H-2K^b and H-2D^d class I antigens and H-2K^b- and H-2D^b-restricted SV40-specific CTL-mediated lysis. *Virology.* 165:357.
5. Burgert, H.-G., J.L. Maryanski, and S. Kvist. 1987. "E3/19K" protein of adenovirus type 2 inhibits lysis of cytolytic T lymphocytes by blocking cell-surface expression of histocompatibility class I antigens. *Proc. Natl. Acad. Sci. USA.* 84:1356.
6. Cox, J.H., J.W. Yewdell, L.C. Eisenlohr, P.R. Johnson, and J.R. Bennink. 1990. Antigen presentation requires transport of MHC class molecules from the endoplasmic reticulum. *Science (Wash. DC).* 247:715.
7. Nuchtern, J.G., J.S. Bonifacino, W.E. Biddison, and R.D. Klausner. 1989. Brefeldin A implicates egress from endoplasmic reticulum in class I restricted antigen presentation. *Nature (Lond.).* 339:223.
8. Yewdell, J.W., and J.R. Bennink. 1989. Brefeldin A specifically inhibits presentation of protein antigens to cytotoxic T lymphocytes. *Science (Wash. DC).* 244:1072.
9. Townsend, A., C. Öhlen, J. Bastin, H.-G. Ljunggren, L. Foster, and K. Kärre. 1989. Association of class I major histocompatibility heavy and light chains induced by viral peptides. *Nature (Lond.).* 340:443.
10. Nilsson, T., M. Jackson, and P.A. Peterson. 1989. Short cytoplasmic sequences serve as retention signals for transmembrane proteins in the endoplasmic reticulum. *Cell.* 58:707.
11. Gooding, L.R., and W.S.M. Wold. 1990. Molecular mechanisms by which Adenoviruses counteract antiviral immune defenses. *Crit. Rev. Immunol.* 10:53.
12. Burgert, H.-G., and S. Kvist. 1987. The E3/19K protein of adenovirus type 2 binds to the domains of histocompatibility antigens required for CTL recognition. *EMBO (Eur. Mol. Biol. Organ.) J.* 7:2019.
13. Jefferies, W.A., and H-G. Burgert. 1991. E3/19K from adenovirus is an immunosubversive protein that binds to a structural motif regulating the intracellular transport of major histocompatibility complex class I proteins. *J. Exp. Med.* 172:1653.
14. Gonatas, J.O., S.G.E. Mezitis, A. Stieber, B. Fleischer, and N.K. Gonatas. 1989. MG-160; A novel sialoglycoprotein of the medial cisternae of the Golgi Apparatus. *J. Biol. Chem.* 264:646.
15. Croul, S., S.G.E. Mezitis, A. Stieber, Y. Chen, J.O. Gonatas, B. Goud, and N.K. Gonatas. 1990. Immunocytochemical visualization of the Golgi apparatus in several species, including human, and tissues with an antiserum against MG-160, a sialoglycoprotein of rat Golgi apparatus. *J. Histochem. Cytochem.* 38:957.
16. Wold, W.S.M., C. Cladaras, S.L. Deutscher, and Q.S. Kapoor. 1985. The 19-kDa glycoprotein coded by the region E3 of adenovirus. *J. Biol. Chem.* 260:2424.
17. Kozak, M. 1989. The scanning model for translation: an update. *J. Cell Biol.* 108:229.
18. Laemmli, U.K. 1970. Cleavage of structural proteins during the assembly of the head of bacteriophage T4. *Nature (Lond.).* 227:680.
19. Bennink, J.R., and J.W. Yewdell. 1988. Murine cytotoxic T lymphocyte recognition of individual influenza virus proteins. *J. Exp. Med.* 168:1935.
20. Degen, E., and D.B. Williams. 1991. Participation of a novel 88-kD protein in the biogenesis of murine class I histocompatability molecules. *J. Cell Biol.* 112:1099.
21. Coupar, B.E.H., M.E. Andrew, D.B. Boyle, and R.V. Blanden. 1986. Immune responses to H-2K^d antigen expressed by recombinant vaccinia virus. *Proc. Natl. Acad. Sci. USA.* 83:7879.
22. Gabathuler, R., and S. Kvist. 1990. The endoplasmic reticulum retention signal of the E3/19K protein of Adenovirus type 2 consists of three separate amino acid segments at the carboxy terminus. *J. Cell Biol.* 111:1803.
23. Jackson, M.R., T. Nilsson, and P.A. Peterson. 1990. Identification of a consensus motif for retention of transmembrane proteins in the endoplasmic reticulum. *EMBO (Eur. Mol. Biol. Organ.) J.* 9:3153.
24. Paabo, S., B.M. Bhat, W.S.M. Wold, and P.A. Peterson. 1987. A short sequence in the COOH-terminus makes an adenovirus membrane glycoprotein a resident of the endoplasmic reticulum. *Cell.* 50:311.
25. Lévy, F., and S. Kvist. 1991. Co-expression of the human HLA-B27 class I antigen and the E3/19K protein of adenovirus-2 in insect cells using a baculovirus vector. *Int. Immunol.* 2:995.
26. Chatterjee, D., and J.V. Maizel. 1984. Homology of adenoviral E3 glycoprotein with HLA-DR heavy chain. *Proc. Natl. Acad. Sci. USA.* 81:6039.
27. Alexander, J., A.J. Payne, B. Shigekawa, J.A. Frelinger, and P. Cresswell. 1990. The transport of class I major histocompatibility complex antigens is determined by sequences in the $\alpha 1$ and $\alpha 2$ protein domains. *Immunogenetics.* 31:169.